J.H. MILLER[1]
Y.A. BAKHIRKIN[2]
T. AJTAI[2]
F.K. TITTEL[2],✉
C.J. HILL[3]
R.Q. YANG[3]

Detection of formaldehyde using off-axis integrated cavity output spectroscopy with an interband cascade laser

[1] Department of Chemistry, The George Washington University, Washington, DC 20052, USA
[2] Department of Electrical and Computer Engineering, Rice University, 6100 South Main Street, Houston, TX 77005-1892, USA
[3] Jet Propulsion Laboratory, California Institute of Technology, 4800 Oak Grove Drive, Pasadena, CA 91109, USA

ABSTRACT A continuous-wave, mid-infrared, distributed feedback, interband cascade laser was used to detect and quantify formaldehyde (H_2CO) using off-axis, integrated cavity output spectroscopy in gas mixtures containing $\approx$ 1–25 parts in 10^6 by volume (ppmV) of H_2CO. Analysis of the spectral measurements indicates that a H_2CO concentration of 150 parts in 10^9 by volume (ppbV) would produce a spectrum with a signal to noise ratio of 3 for a data acquisition time of 3 s. This is a relevant sensitivity level for formaldehyde monitoring of indoor air, occupational settings, and on board spacecraft in long duration missions in particular as the detection sensitivity improves with the square root of the data acquisition time.

PACS 07.07.Df; 82.80.Ch

1   Introduction

1.1   *Formaldehyde and its detection*

Formaldehyde (H_2CO) is widely used in the manufacture of building materials and numerous household products. Out gassing of formaldehyde from these materials may lead to elevated indoor air levels particularly for poorly ventilated structures. It is also an important intermediate in the oxidation of hydrocarbons in both combustion systems and in the troposphere. Thus, H_2CO may be present in substantial concentrations in both indoor and outdoor air samples.

Tropospheric H_2CO concentration measurements provide a means of validating photochemical model predictions that play a key role in our understanding of tropospheric ozone formation chemistry [1]. Formaldehyde is a pungent-smelling, colorless gas that causes a variety of effects (including watery and/or burning eyes, nausea, and difficulty in breathing) in some humans exposed to H_2CO levels of only 100 ppbV. Known to cause cancer in animals, it is also a suspected human carcinogen.

Formaldehyde is detected by odor by humans ranging from concentrations of 0.07 to 1.2 ppmV in air. The Occupational Safety and Health Administration has established permissible exposure limit (PEL) of 0.75 ppmV averaged for an eight-hour work day and short term exposure limit (STEL) of 2 ppmV averaged over 15 min [2]. At levels ten times the PEL, respiratory protection is required. Other organizations have taken a more conservative approach to formaldehyde management. For example, the threshold limit value (TLV) for H_2CO established by the American Conference of Governmental Industrial Hygienists is 0.3 ppmV as a "ceiling limit" not to be exceeded at any time, and has classified it as a "suspected human carcinogen". A committee of the National Academy of Sciences, working on behalf of NASA, has extensively reviewed the toxicity of formaldehyde and has established spacecraft maximum allowable concentrations for various times of exposure [3]. Their recommended upper limits range from 0.4 ppmV for short term (1 h) exposure down to 0.04 ppmV for seven to 180 day space missions.

To quantify H_2CO concentrations, several different chemical [4, 5] and physical detection methods have been used. Chemical analyzers, which employ coloration of a formaldehyde-sensitive reagent, are sensitive at ppbV levels but they suffer from cross-interference effects by other aldehydes and require long sampling times (i.e., minutes or more). To overcome these limitations, laser-based spectroscopic sensors have been developed. Several different tunable, cw laser sources have been employed to access H_2CO absorption lines, including lead-salt lasers [6, 7], difference frequency generation (DFG) [8] sources, CO overtone gas lasers [9], and optical parametric oscillators (OPOs) [10, 11]. The best H_2CO detection sensitivity reported [12] (< 50 pptv for a 1 minute integration time) was achieved using lead salt diode laser-based absorption spectroscopy in a multipass optical cell with an effective optical path length of 100 m.

The emphasis of the work reported here is the demonstration of cavity-enhanced absorption of formaldehyde at concentrations appropriate for indoor air monitoring. A sensor based on the principles demonstrated here would potentially be small in volume, relatively immune to mechanical perturbation, and would have modest requirements for electronic control circuitry. In the sections that follow, we will introduce the mid-infrared sources and sensing strategy used in this study.

✉ Fax: +1-713-348-5686, E-mail: fkt@rice.edu

1.2   *Interband cascade lasers*

Recently, distributed feedback (DFB) interband cascade lasers (ICLs) [13, 14] have been constructed that can access wavelengths between 3 and 4 µm [15], a spectral region which has been difficult to cover with intraband quantum cascade lasers (QCLs). ICLs employ transitions between the conduction and valence bands as in bipolar diode lasers, but instead of losing an electron to the valence band it is recycled through interband tunneling into the conduction band of the next cascade stage. This is made possible with the type-II broken gap alignments in InAs/GaInSb quantum well structures. Because the conduction and valence bands have opposite dispersion curvatures, fast phonon scattering loss is circumvented in ICLs, which results in a more efficient operation with a low threshold current density. The emission wavelength of ICLs can be tailored in a wide spectral range, particularly on the shorter-wavelength side due to a large band offset between their constituent materials. Recently, continuous-wave (cw) operation of ICLs have been demonstrated at JPL at temperatures up to 264 K. It is likely that cw operation of ICLs at room-temperature will be achieved soon by improving design and thermal management on the current devices [13].

1.3   *Integrated cavity output spectroscopy*

Absorption spectra resulting from methods such as tunable diode laser absorption spectroscopy (TDLAS) with wavelength or frequency modulation, and FTIR are typically easy to interpret and are not limited by species selectivity. However, to gain the sensitivities required to be competitive with such as GC/MS or laser induced fluorescence (LIF), very long pathlength are required which results in large volume instruments. Cavity ringdown spectroscopy (CRDS) is a sensitive absorption technique that is capable of monitoring a wide range of species [16–19] in modest-sized instrument packages. In cw-CRDS, a beam from the diode laser is injected into an optical cavity formed between two highly reflective mirrors. Only light with a frequency that matches a cavity transmission mode is coupled into the cavity due to constructive interferences. The energy of light at these resonant frequencies builds up in the cavity over time. When the energy reaches a set threshold, the input beam is shut off and a ringdown is recorded. The CRDS technique, while very sensitive, depends on fast electronics both for shuttering and for the data acquisition process needed to capture and store the ringdown waveform that is on the order of microseconds.

Integrated cavity output spectroscopy (ICOS) provides enhanced cavity sensitivity using a less complex setup than CRDS [20, 21]. In CRDS it is desirable to only excite the TEM$_{00}$ mode of the laser into the cavity. This is due to the fact that transverse modes sample a greater portion of the mirror surface. Inhomogeneities in mirror reflectivity lead to variation in ring-down time constants. With ICOS, the transmitted output of the cavity is time-integrated to provide an absorption spectrum as the wavelength is scanned through the region of interest. The spectrum is then converted to absorbance through the Beer–Bougert–Lambert Law. Off-axis ICOS (OA-ICOS), in which the laser beam is directed at an angle with respect to the cavity axis, provides increased spectral density of cavity modes and thus minimizes the noise in the resulting absorption spectra [21, 22]. A higher order transverse mode, designated by TEM$_{mn}$, has a $m + n$ times smaller free spectral range compared with the TEM$_{00}$ mode. Off-axis excitation excites many of these higher order modes, thus providing near continuous excitation of the cavity as the wavelength of the ICL source is tuned. Further, mechanical vibrations serve to randomize coupling modes further, leading to more continuous spectral throughput. As a result, OA-ICOS approach is more immune to mechanical instability than CRDS technique.

1.4   *Spectroscopy theory and data analysis*

Typically, in an absorption measurement, the decrease in light amplitude through an absorber is measured. The Beer–Bougert–Lambert Law gives the magnitude of the absorption:

$$\frac{I}{I_0} = \exp^{-Sg\varrho x_J l} = \exp^{-\alpha l}, \tag{1}$$

where S is the line strength of the absorption, g is a line shape factor, ϱ is the gas density, x_J is the mole fraction of the absorber, l is the pathlength though the absorber, and α is the extinction coefficient. For an ICOS experiment, the laser power transmitted through the optical cavity is given by [21]

$$I = I_0 C_p \frac{(1-R)^2}{2[(1-R) + \alpha l]}, \tag{2}$$

where R is the reflectivity of the mirrors and C_p is a spatial coupling parameter assumed to range from 0 to 1. Of course, coupling is never perfect and, as noted above, reflectivity for higher-order modes is lower than that of the TEM$_{00}$ mode. Cast in terms of the effective reflectivity, R_{eff}, the fractional absorption is then given by:

$$A = \frac{\alpha l}{[(1 - R_{\text{eff}}) + \alpha l]}. \tag{3}$$

The effective reflectivity can be obtained through a measurement of the cavity ring down time or, as demonstrated below, by first determining the effective pathlength of the measurement, P_{eff}, and calculating $R_{\text{eff}} = 1 - l/P_{\text{eff}}$.

2   **Experimental**

A schematic of the apparatus used in this study is shown in Fig. 1. The optical arrangement and electronic control of the experiment for ICOS is similar to that published previously by the Rice Laser Science Group for measurement of NO at 1835 cm^{-1} using a quantum cascade laser [23]. The interband cascade laser used is identical to that described in a recent publication in which formaldehyde was measured utilizing quartz-enhanced photo acoustic spectroscopy [24]. Briefly, light from a cooled ICL was collimated using a 12.5 mm f.l. ZnSe lens and directed into an ICOS cell. Downstream output from the ICOS cell was collected with an off-axis parabolic mirror (75 mm diameter; 75 mm f.l.) and detected with an InSb detector (Judson Technologies).
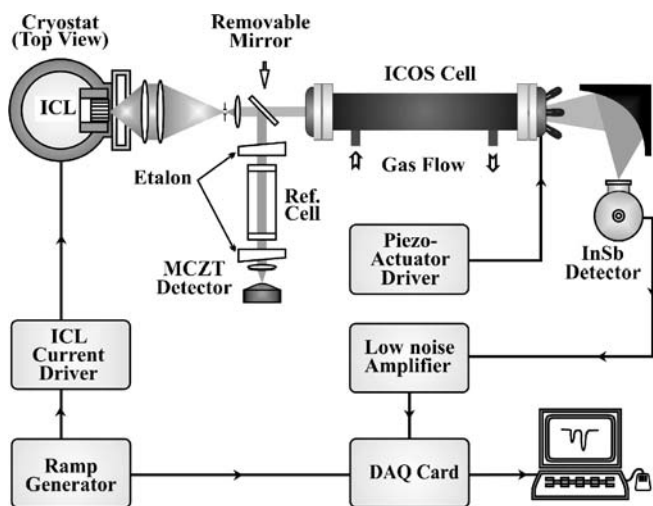
FIGURE 1 Experimental arrangement used in OA-ICOS detection of formaldehyde

The ICL, housed in a liquid-nitrogen cryostat (Cryo Industries, Inc.), provided output powers of up to 12 mW at 3.53 μm. The output is tunable from 2831.8 cm^{-1} to 2833.7 cm^{-1} by varying the injection current. The low threshold current operation of ICLs requires a current source with relatively high precision (an ILX Lightwave model LDX 3220 was used in this study).

The specific ICL used in this work is able to operate continuously up to 170 K. At or near liquid nitrogen temperatures, the laser operates with a bias voltage of $\approx$ 7–8 V and a relatively low threshold current of approximately 3 mA. Although

the output of the DFB ICL laser is nominally single mode, other weaker modes are apparent in the spectrum of the laser output at $\approx$ 2840, 2851, and 2866 cm^{-1} whose power can be up to $\approx$ 4%, 2%, and 1% of the power of the 2832 cm^{-1} mode. Figure 2 shows schematically how the ICL output power is distributed among the modes when tuned from near threshold up to an injection current of approximately 25 mA. Figure 3 illustrates how these modes coincide with formaldehyde lines in the mid 2800 cm^{-1} spectral region. As this figure shows, spectral lines in the range of the 2nd most powerful mode near 2840 cm^{-1} are substantially weaker than those excited by the primary mode. Even so, several unidentified, weaker features were observed in the ICOS spectrum of H_2CO that may be attributable to excitation of secondary modes. Of course, spectral filtering of the laser output or improvement in the DFB grating structure of the ICL can eliminate the side band mode structure.

With the ICL operating at $\approx$ 80 K, it is possible to access several formaldehyde absorption lines. Figure 4 shows a simulation of the spectral region available for analysis under the approximate conditions employed in formaldehyde quantification. Also shown are the relative line strengths from the HITRAN database that range from 1×10^{-20} to 5×10^{-20} cm^{-1}/(molecule cm^{-2}). Apparent in the spectrum in this figure is the fact that some of the observed features are blends of several rovibrational lines. Of the two isolated features in this spectrum (2832.483 cm^{-1}, $7_{0,7} \leftarrow 6_{1,6}$, and 2833.191 cm^{-1}, $6_{0,6} \leftarrow 6_{1,5}$, of the ν_5 fundamental), we chose to exploit the OA-ICOS signal of the former, indicated with a triangle in Fig. 4, for quantitative analysis.
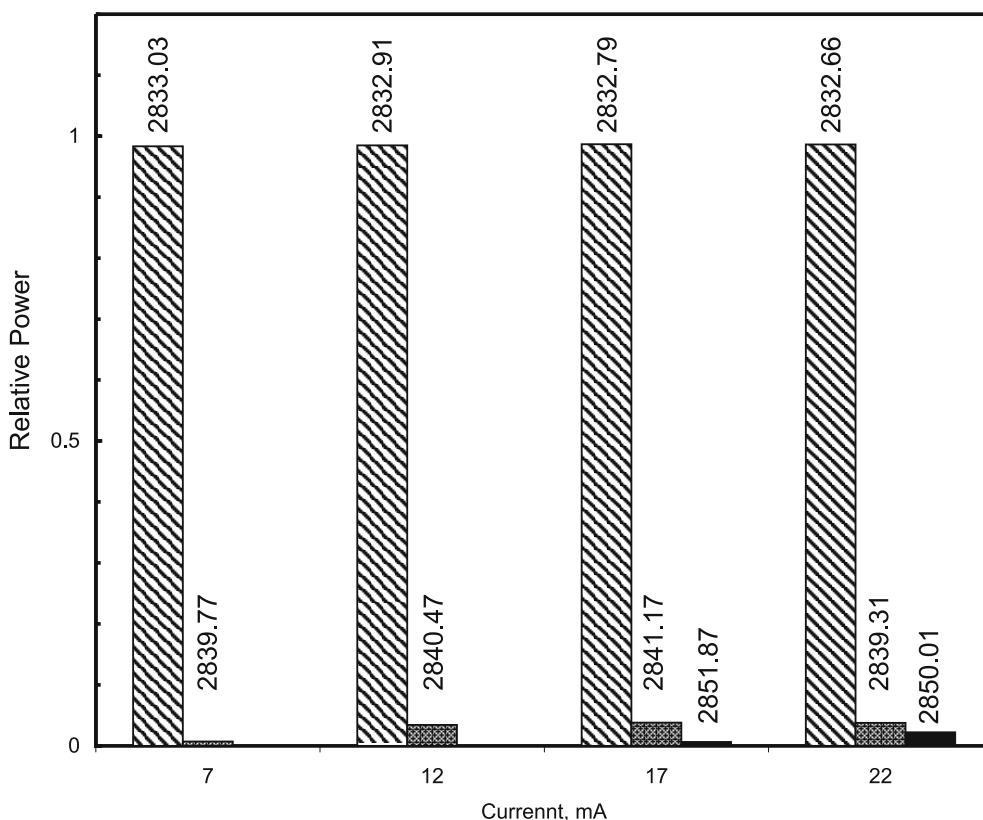

FIGURE 2 Mode structure of ICL used in this study. Increasing current leads to increasing power in side bands
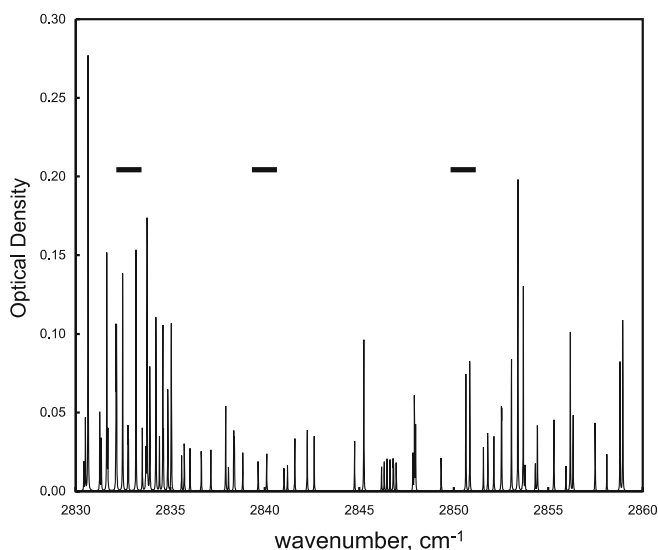
FIGURE 3 Simulation of formaldehyde spectrum at ~ 2832 cm^{-1} in the mid-infrared region. For this simulation, formaldehyde concentration was assumed to be 25 ppmV, the pressure was 50 Torr, the temperature was 296 K, and the pathlength was 20 m. *Horizontal line segments* show wavenumbers of ICL modes (see Fig. 2)

A gas standard generator (Kin-Tek model 491M) based on a permeation tube was used to provide H_2CO concentrations ranging from 0.5 to 25 ppmV in the diluting gas nitrogen. To minimize the effects of formaldehyde stickiness, ultra pure perfluoroalkoxy tubing was used for all gas handling. Further, to eliminate memory effects spectra were collected in ascending concentrations ranging from ≈ 1 to 25 ppmV. In a typical experiment the formaldehyde gas mixture was introduced into a custom, 50 cm long, ≈ 650 cm^3 OA-ICOS cell equipped with 50 mm diameter, high reflectivity mirrors (Novawave Technology). Cell pressure was maintained with a pressure controller (MKS Instruments type 659) at 50 Torr. The flow rate necessary to maintain this pressure varied from

50 to 100 sccm. Cavity modes were randomized by imposing a continuous, ≈ 200-Hz modulation on one set of the cavity mirrors using three piezo actuators.

Spectra were collected by ramping the laser current at 300 Hz to cover the spectral region shown in Fig. 4 (≈ 20 mA) and collecting the detector output using a data acquisition system connected to a personal computer and controlled by LabView 6.1 software. The sampling rate for the digitizer was 0.5 Msample/s. Thus, each scan consisted of approximately 1667 data points (≈ 200 points per spectral feature). By beginning the current scans below the threshold for lasing, a "zero" laser level for the AC coupled detector signal could be established. Typically, 1000 spectral scans (for a total measurement time of 3.3 s) were averaged for each formaldehyde determination. Three such averaged spectra were collected for each formaldehyde concentration.

3   Results and discussion

Figure 5 shows part of the OA-ICOS spectrum for a 26.57 ppmV mixture of formaldehyde in nitrogen centered on the 2832.483 cm^{-1} feature. Also shown is a fit of the data using a Voigt line shape function. For the latter, line shape parameters (collision width, temperature and pressure dependencies, etc.) were taken from the 2000 version of the HITRAN database [25]. There are no significant changes in the formaldehyde spectral line properties in this spectral region in the 2004 version of the database. Although the determination of concentrations through background correction and line fitting was done off line here, there is in principle no reason that this could not be done in real time using integrated DSP technology.

The effective optical pathlength, P_{eff}, was determined from a fit of the experimental spectrum for 1 ppmv of formaldehyde in the cell. The discrepancy between the estimated ($R_{eff} \sim 99.4\%$) reflectivity and that specified by the manufacturer ($R \sim 99.95\%$, which was most likely derived
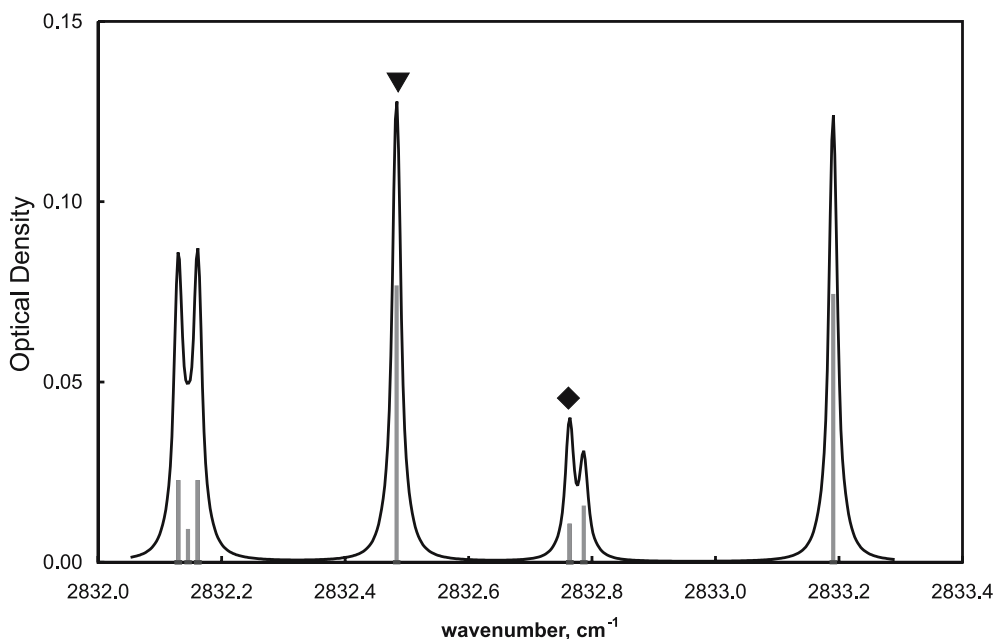

FIGURE 4 Simulation of formaldehyde spectrum in the spectral region available by the ICL used in this study. The line at 2832.485 cm^{-1}, marked with a *triangle*, was used for H_2CO quantification. The feature marked with a *diamond* is a doubly degenerate line pair. Line positions from the HITRAN database are shown as *vertical lines* whose relative strength is indicated by height
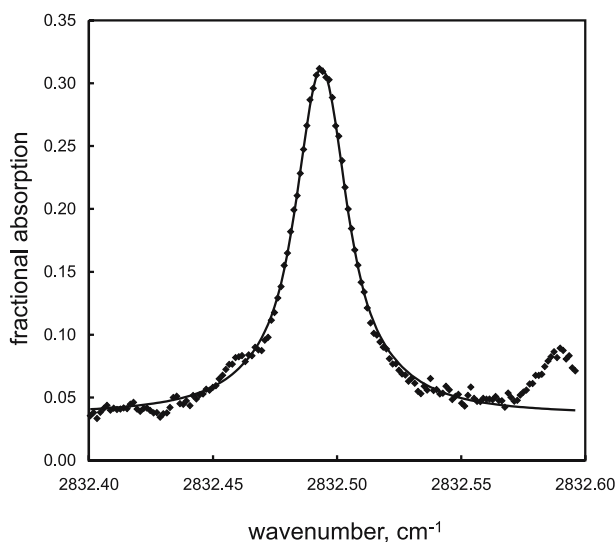
FIGURE 5   *Symbols*: Experimental spectrum of the 2832.485 cm^{-1} line at a formaldehyde concentration of 26.57 ppmV. *Line*: fit of data using HITRAN line parameters and a Voigt line shape
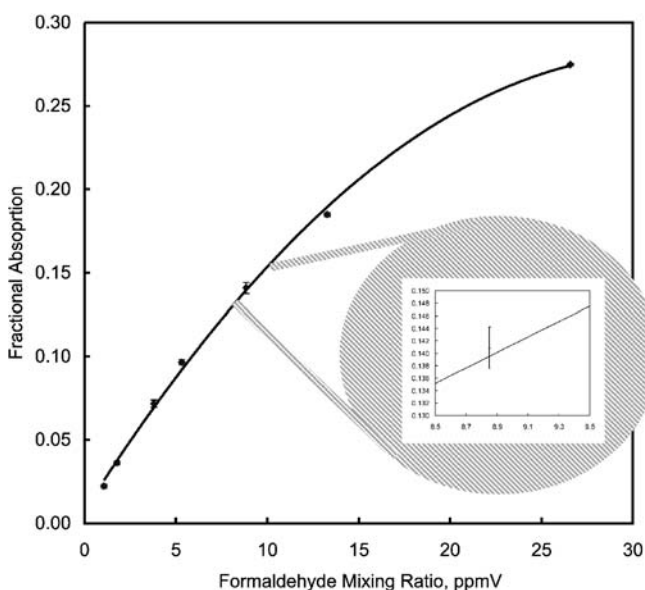

FIGURE 7   *Symbols*: Experimental spectrum of the 2832.485 cm^{-1} line at a formaldehyde concentration of 1 ppmV. *Line*: fit of data using HITRAN line parameters and a Voigt line shape. The one standard deviation level in the residuals of the fit was found to be equivalent to a concentration of 50 ppbV

FIGURE 6   Dependence of fractional absorption on formaldehyde concentrations. Several spectra were acquired at each concentration. *Error bars* (barely discernible here) show standard deviations within the fits for these groups. *Inset* shows one standard deviation for one of these determinations

from the cavity ring-down time for the TEM$_{00}$ mode) is due to several factors including: 1) non-homogeneity of the reflectivity across the 2 inch diameter mirror surfaces, 2) a large number of higher order transverse modes that are coupled in OA-ICOS measurements which have larger diffraction losses than for the TEM$_{00}$ mode, and thus lower effective optical pathlength, and 3) tilting of the PZT driven mirror which affects the OA-ICOS cavity alignment and, therefore, results in a decrease of the cavity finesse.

Figure 6 shows the dependence of the fractional absorption at line center on formaldehyde concentration. In the inset of Fig. 6 is shown the standard deviation for the three measurements at 10 ppmV of formaldehyde demonstrating the high precision in these measurements. The average of the standard deviations for each concentration in the frac-
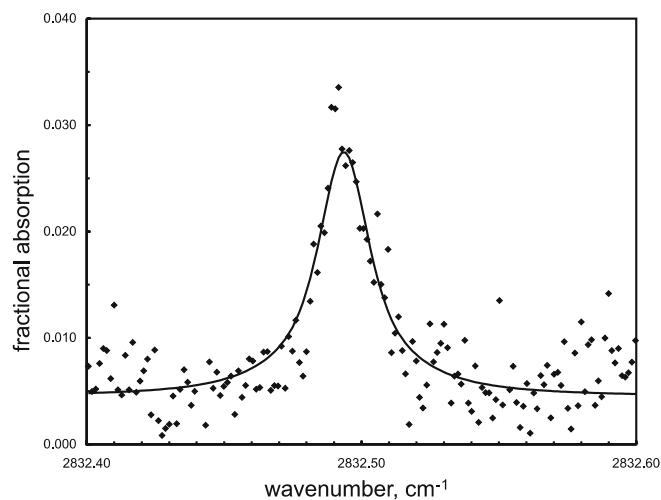
tional absorption calibration curve was 0.15%, equivalent to a formaldehyde detection limit of < 100 ppbV.

An alternative calculation of the detection limit is available by considering the standard deviation in an individual fit of a spectrum. Figure 7 shows the fit of a spectrum collected for 1 ppmV of formaldehyde in nitrogen mixture. From the residuals trace in this fit, the one standard deviation concentration of formaldehyde is estimated at ≈ 50 ppbV. Thus, a H$_2$CO concentration of 150 ppbV would produce a spectrum with a signal to noise ratio of 3. It is worth noting that the sensitivity in an ICOS measurement decreases with the square root of the integration time. Thus, we would anticipate that an increase in the scanning ramp frequency and/or the sampling time by two orders of magnitude would decrease the detection limit to 15 ppbV.

4   Conclusions

We have demonstrated the off-axis integrated cavity output spectroscopy of formaldehyde at a detection limit of 150 ppbV (SNR = 3). As noted in the introduction, this is a relevant level for formaldehyde monitoring in indoor air, occupational settings, and on board of spacecrafts in long duration missions. Because ICOS can be performed with low volume sample cells and is more immune to mechanical vibration than other cavity enhanced absorption techniques, this technology is an attractive choice for sensor development with emerging mid infrared sources.

REFERENCES

1 B.P. Wert, M. Trainer, A. Fried, T.B. Ryerson, B. Henry, W. Potter, W.M. Angevine, E. Atlas, S.G. Donnelly, F.C. Fehsenfeld, G.J. Frost,

P.D. Goldan, A. Hansel, J.S. Holloway, G. Hubler, W.C. Kuster, D.K. Nicks, J.A. Neuman, D.D. Parrish, S. Schauffler, J. Stutz, D.T. Sueper, C. Wiedinmyer, A. Wisthaler, J. Geophys. Res. **108**, ACH8/1 (2003)

2 OSHA Standards – 29 CFR 1910.1048 (2006)

3 R.E. Crossgrove, *Spacecraft Maximum Allowible Concentrations for Selected Airborne Contaminants* (National Academy of Sciences, 1994–2000), Vol. 1–4

4 J.R. Hopkins, T. Still, S. Al-Haider, I.R. Fisher, A.C. Lewis, P.W. Seakins, Atmos. Environ. **37**, 2557 (2003)

5 Y. Suzuki, N. Nakano, K. Suzuki, Environ. Sci. Technol. **37**, 5695 (2003)

6 D. Richter, P. Weibring, Appl. Phys. B **82**, 479 (2006)

7 P. Weibring, D. Richter, A. Fried, J.G. Walega, C. Dyroff, Appl. Phys. B (2006), unpublished, DOI: 10.1007/s00340-006-2300-4

8 D.G. Lancaster, A. Fried, B. Wert, B. Henry, F.K. Tittel, J. Appl. Opt. **39**, 4436 (2000)

9 H. Dahnke, G. von Basum, K. Kleinermanns, P. Hering, M. Mürtz, Appl. Phys. B **75**, 311 (2002)

10 F. Müller, A. Popp, F. Kühnemann, S. Schiller, Opt. Express **11**, 2820 (2003)

11 M.M.J.W. van Herpen, S.E. Bisson, A.K.Y. Ngai, F.J.M. Harren, Appl. Phys. B **78**, 281 (2004)

12 P. Wert, A. Fried, S. Rauenbuehler, J. Walega, B. Henry, J. Geophys. Res. **108**, ACH1/1 (2003)

13 R.Q. Yang, C.J. Hill, B.H. Yang, Appl. Phys. Lett. **87**, 151 109 (2005)

14 R.Q. Yang, C.J. Hill, Y. Qiu, Mater. Res. Soc. Symp. Proc. **891**, 0891-EE01-06 (2006)

15 R.Q. Yang, C.J. Hill, B.H. Yang, C.M. Wong, R.E. Muller, P.M. Echternach, Appl. Phys. Lett. **84**, 3699 (2004)

16 D. Romanini, Ann. Phys. (Paris) **20**, 665 (1995)

17 D. Romanini, A.A. Kachanov, N. Sadeghi, F. Stoeckel, Chem. Phys. Lett. **264**, 316 (1997)

18 B.A. Paldus, J.S. Harris Jr., J. Martin, J. Xie, R.N. Zare, J. Appl. Phys. **82**, 3199 (1997)

19 J.H. Miller, A. R Awtry, M. E Moses, A.D. Jewell, E.L. Wilson, Proc. Combust. Inst. **29**, 2203 (2002)

20 A. O'Keefe, J.J. Scherer, J.B. Paul, Chem. Phys. Lett. **307**, 343 (1999)

21 Y.A. Bakhirkin, A.A. Kosterev, C. Roller, R.F. Curl, F.K. Tittel, Appl. Opt. **43**, 2257 (2004)

22 J.B. Paul, L. Lapson, J.G. Anderson, Appl. Opt. **40**, 4904 (2001)

23 Y.A. Bakhirkin, A.A. Kosterev, R. Curl, F.K. Tittel, D.A. Yarekha, L. Hvozdara, M. Giovannini, J. Faist, Appl. Phys. B **82**, 149 (2006)

24 M. Horstjann, Y.A. Bakhirkin, A.A. Kosterev, R.F. Curl, F.K. Tittel, C.M. Wong, C.J. Hill, R.Q. Yang, Appl. Phys. B **79**, 799 (2004)

25 L.S. Rothman, A. Barbe, D. Chris Benner, L.R. Brown, C. Camy-Peyret, M.R. Carleer, K. Chance, C. Clerbaux, V. Dana, V.M. Devi, A. Fayt, J.M. Flaud, R.R. Gamache, A. Goldman, D. Jacquemart, K.W. Jucks, W.J. Lafferty, J.Y. Mandin, S.T. Massie, V. Nemtchinov, D. A Newnham, A. Perrin, C.P. Rinsland, J. Schroeder, K.M. Smith, M.A.H. Smith, K. Tang, R.A. Toth, J. Vander Auwera, P. Varanasi, K. Yoshino, J. Quantum Spectrosc. Radiat. Transf. **82**, 5 (2003)